Efficient finite element modeling of photonic structures with combined symmetry operations for waveguide modal analysis

line 1: Jingwei Wang
line 2: *School of Optical and Electronic Information*
line 3: *Huazhong University of Science and Technology*
line 4: Wuhan, China
line 5: d202080780@hust.edu.cn

line 1: Lida Liu
line 2: *School of Optical and Electronic Information*
line 3: *Huazhong University of Science and Technology*
line 4: Wuhan, China
line 5: m202373096@hust.edu.cn

line 1: Yuntian Chen
line 2: *School of Optical and Electronic Information*
line 3: *Huazhong University of Science and Technology*
line 4: Wuhan, China
line 5: yuntian@hust.edu.cn

***Abstract*—Symmetry is widely used to analyze the optical properties of photonic devices, which can improve the efficiency and accuracy of full-wave simulations. Existing optical full-wave simulations mostly use a single symmetry to simplify the calculations. In this work, we lay out the theoretical foundation and numerical implementation of the finite element method (FEM) that combines various symmetry operations, significantly improving the computational efficiency. Our method integrates multiple spatial or non-spatial symmetry operations, decomposing the original problem into several decoupled sub-problems for analyzing the vector eigenmodes of photonic devices. We employ our proposed method to compute the vector eigenmodes of two-dimensional optical waveguides and conduct a comparative analysis against the standard FEM. The obtained results demonstrate excellent agreement between our method and std. FEM while simultaneously showcasing enhanced computational efficiency multiple times at least. Furthermore, our method classifies the eigenmodes directly based on symmetry, with one category of eigenmode corresponding to one sub-task, which is beneficial for analyzing and designing waveguide modal characteristics.**

Keywords—symmetry, finite element method, modal analysis

I. INTRODUCTION

Symmetry is widely used to qualitatively analyze the optical properties of photonic devices, and also quantitatively to study photonic devices with enhanced efficiency and accuracy using full-wave simulations. For instance, symmetry has been used to enhance optical nonlinearity[1] , to analyze and classify waveguide modes[2], and to design symmetry protected photonic topological edge states[3] or the construction of coupled mode theory[4]. Meanwhile, symmetry can simplify numerical calculations of photonic devices and reduce computational complexity in computational photonics. Indeed, mirror-symmetric optical devices has been routinely truncated using perfect electric conductor (PEC) or perfect magnetic conductor (PMC) conditions to halve the computational domain[5]. As for calculating the eigenmodes of photonic devices with c_N symmetry, the calculation domain can be truncated into 1/N using rotational Bloch boundary conditions[6].

Notably, aforementioned studies on simplifying photonic device calculations through symmetry mainly focus on a single symmetry. In contrast, many photonic devices intrinsically possess multiple symmetries. In recent years, there has been significant progress in leveraging multiple symmetry operation to reduce the computational complexity of device dynamics. Little effort on taking advantage of symmetry arguments have been made in computational photonics. Theoretically, it is also possible to combine multiple symmetry operations to further simplify the computational complexity when numerically calculating the optical properties of photonic devices[7]. When combining symmetry operations, it is crucial to consider that the same symmetry imposes different constraints on different types of eigenmodes in computational photonics i.e., different reducible representations in the language of group theory. For instance, the application of mirror symmetry on electric fields presents two distinct cases: symmetric and anti-symmetric, which differ from dynamics. Determining how to choose the combined symmetry operations and their constraints to ensure the solution of all types of eigenmodes is not straightforward and has never been examined thoroughly in self-consistent manner.

In this paper, we study the photonic device with multiple symmetry operation. We thoroughly revisit the utilization of symmetry in FEM introducing by group theory. It allows for the classification of photonic device eigenmodes based on their symmetry and provides a mathematical description of the symmetry exhibited by the eigenmodes[8], [9]. We show that the combination of multiple symmetries can facilitate the decomposition of the original eigenmode problem into several sub-problems, each capable of computing a specific class of vector eigenmodes. This decomposition not only streamlines the analysis of photonic device modes but also reduces computation time compared to the original problem. Because our method classifies modes based on symmetry before solving, it can calculate specific categories of modes only, which provides a comprehensive approach for waveguide analysis and modal characteristic design. The framework proposed in this paper includes the widely used method of truncating the calculation domain through two kinds of mirror symmetry, and extends to the combination of rotational symmetry, and even space-time symmetry. Additionally, we have illustrated that different sub-problems can be concurrently computed, resulting in significant improvements in computational efficiency. Although the exploration of parallel computation is beyond the scope of this paper, there is no doubt that parallel computation in combination with our

2024 Light Conference (LCW) | 979-8-3503-9227-2/24/$31.00 ©2024 IEEE | DOI: 10.1109/LCW63366.2024.10776583

method can further speed up the computational process if multiple symmetry types exist.

II. Theory and Methods

A. Symmetry operation and character table

The eigenmode of photonic devices satisfy the vector wave equation,

$$\nabla\times\boldsymbol{\mu}_r^{-1}\nabla\times\mathbf{E}(\mathbf{r})-k_0^2\boldsymbol{\epsilon}_r\mathbf{E}(\mathbf{r})=0, \quad (1)$$

where ∇ is the del operator, μ_r is the relative permeability, ϵ_r is relative permittivity, k_0 is the wave number in vacuum, and $\mathbf{E}(\mathbf{r})$ is the eigenmode field. In the waveguide modal analysis, the transverse and longitudinal components of the electric field can be separated and written as $\mathbf{E}(\mathbf{r})=[\mathbf{E}_t(x,y)+\hat{z}E_z(x,y)]e^{-\gamma z}$, where $\gamma=\alpha+j\beta$ is the complex propagation constant. In group theory, the matrix corresponding to the spatial symmetry O is denoted as $\hat{O}$, and the corresponding symmetric operator is P_O . If $\hat{O}\boldsymbol{\epsilon}_r\left(\hat{O}^{-1}\mathbf{r}\right)\hat{O}^{-1}=\boldsymbol{\epsilon}_r(\mathbf{r})$, $\hat{O}\boldsymbol{\mu}_r\left(\hat{O}^{-1}\mathbf{r}\right)\hat{O}^{-1}=\boldsymbol{\mu}_r(\mathbf{r})$, then the photonic device has O spatial symmetry. When the device has O spatial symmetry, the eigenmodes of the device will also have the same symmetry, $P_O\mathbf{E}(\mathbf{r})=\chi(O)\mathbf{E}(\mathbf{r})=\hat{O}\mathbf{E}(\hat{O}^{-1}\mathbf{r})$, that is,

$$\chi(O)\mathbf{E}(\mathbf{r})=\hat{O}\mathbf{E}(\hat{O}^{-1}\mathbf{r}), \quad (2)$$

where $\chi(O)$ is the character of symmetry O and describes the constraints of symmetry on different classifications of eigenmodes. The collection of all spatial symmetry operations in a non-periodic photonic device is referred to as the point group. The character table of point group classifies the eigenmodes and lists the characters of all symmetry operations acting on each class of modes. Table I shows the character table corresponding to the $C_{2,v}$ point group, which classifies the eigenmodes of photonic devices with $C_{6,v}$ symmetry into six different types, i.e., A_1, A_2, B_1, B_2, E_1, and E_2. E_1 and E_2 are degenerate modes. From the character table, it can be deduced that the eigenmodes of this device possess rotational symmetry and mirror symmetry. The mirror symmetry operator σ_v has a mirror symmetric effect on mode A_1, $P_{\sigma_v}A_1=\chi(\sigma_v)A_1$, where the character $\chi(\sigma_v)=1$. The mirror symmetry operator σ_v has a mirror anti-symmetric effect on mode A_2, $P_{\sigma_v}A_2=\chi(\sigma_v)A_2$, where the character $\chi(\sigma_v)=-1$. The mode categories in Table I have specific corresponding relationships with the LP modes of the waveguide[2].

TABLE I. Character Table for $\mathbf{C_{6,v}}$ Point Group Table Type Styles

	E	$2C_6$	$2C_3$	C_2	$3\sigma_v$	$3\sigma_d$
A_1	1	1	1	1	1	1
A_2	1	1	1	1	-1	-1
B_1	1	-1	1	-1	1	-1
B_2	1	-1	1	-1	-1	1
E_1	2	1	-1	-2	0	0
E_2	2	-1	-1	2	0	0

Based on the classification of modes by character tables, we can decompose the initial eigenvalue problem of photonic devices into multiple sub-eigenvalue problems using symmetry, each sub-eigenvalue problem calculates a class of modes. Since each class of mode corresponds to an irreducible representation in the character table, all sub-eigenvalue problems are complete and completely decoupled. Using character table, we can classify and select the appropriate symmetries and their character in order to calculate all the eigenmodes of the photon device without omission. When selecting symmetries, it is important to consider that the combined symmetry can be applied in the same truncation domain and to minimize the size of the truncation domain. Point group only includes spatial symmetries, while some space-time symmetries, such as MT symmetry[10], can also be combined with spatial symmetries to further truncate the calculation domain. Therefore, when using combined symmetry operations to truncate the calculation domain of photonic devices, this paper discusses two cases: one is to only use point group symmetries, and the other is to use space-time symmetry symmetries.

B. Combination of point group symmetries

When only using point group symmetries, the symmetries are selected, and constraints are imposed on the eigenmodes based on the character table. In the two-dimensional point group, there are only two symmetries: rotational symmetry and mirror symmetry. Therefore, in this case, the calculation domain can only be truncated by using the combination of rotational and mirror symmetries. Taking an example of the $C_{N,v}$ (N>2) point group symmetric structure, selecting the rotational symmetry C_N and the mirror symmetry σ_v minimizes the truncation domain. The matrix corresponding to rotational symmetry C_N is $\hat{R}(\theta)=\begin{pmatrix}\cos\theta & -\sin\theta & 0\\ \sin\theta & \cos\theta & 0\\ 0 & 0 & 1\end{pmatrix}$, and The matrix corresponding to mirror symmetry σ_v is $\hat{S}(\theta)=\begin{pmatrix}\cos 2\theta & \sin 2\theta & 0\\ \sin 2\theta & -\cos 2\theta & 0\\ 0 & 0 & 1\end{pmatrix}$. From (2), the rotational symmetry C_N imposes constraints on the eigenmode as follows,

$$\chi(C_N)\mathbf{E}(\mathbf{r})=\hat{R}\left(\frac{2\pi}{N}\right)\mathbf{E}\left(\hat{R}^{-1}\left(\frac{2\pi}{N}\right)\mathbf{r}\right). \quad (3)$$

The constraint of mirror symmetry σ_v on the non-degenerate modes is as follows,

$$\chi(\sigma_v)\mathbf{E}(\mathbf{r})=\hat{S}(\theta)\mathbf{E}\left(\hat{S}^{-1}(\theta)\mathbf{r}\right). \quad (4)$$

The constraint of mirror symmetry σ_v on the degenerate modes is as follows,

$$\mathbf{E}(\mathbf{r})=\hat{S}(\theta)\mathbf{E}^*\left(\hat{S}^{-1}(\theta)\mathbf{r}\right). \quad (5)$$

By utilizing (3), (4), and (5), combined symmetric boundary conditions can be obtained for truncating the calculation

domain. It should be noted that the method of truncating the calculation domain with respect to the mirror symmetry about the x-axis and the mirror symmetry about the y-axis, which is currently widely used in FEM, is included in our method framework. That is, C_{2v} point group and its character table are used to build boundary constraints. The use of two mirror symmetry to truncate the calculation domain is a special case of combined symmetric boundary conditions, and it is only applicable to the case of using C_{2v} point group symmetry. When $C_{N,v}(N>2)$ point group symmetry is used, only mirror symmetry cannot describe the constraints on degenerate modes, and the combination of rotational symmetry and mirror symmetry must be used.

C. *Combination of point group symmetry and space-time symmetry*

When utilizing space-time symmetry, it is still necessary to select the symmetry and impose constraints on the eigenmodes based on the character table. Meanwhile, all classifications of eigenmodes in the character table satisfy space-time symmetry. Therefore, it is only necessary to select the symmetry that can combine with space-time symmetry from the character table to construct constraints on the eigenmodes. Taking a structure with C_N point group and MT symmetry as an example, we choose rotational symmetry c_N and MT symmetry to truncate the domain. The rotational symmetry c_N still satisfies (3) for the eigenmode field constraints, and the MT symmetry imposes constraints on the eigenmodes that satisfies (5). By employing (3) and (5), one can obtain the combined symmetric boundary conditions used for truncating the calculation domain.

III. Results and Discussions

To verify the effectiveness of the method proposed in this paper, we analyze through the numerical example of a complex two-dimensional photonic crystal waveguide. The case of point group symmetry will be illustrated using the $C_{N,v}$ point group symmetry structure as an example, while the case of space-time symmetry will be illustrated using the C_N point group and MT symmetry structure as an example. Based on the symmetry employed, we label the two discussed cases as $C_{N,v}$-FEM and $C_{N,\sigma_v T}$-FEM. All numerical results are obtained by MATLAB with home-made code. In this paper, the mesh density is denoted as S, and the maximum element size is set to $\frac{\lambda}{S}$, where λ is the wavelength. To compare the accuracy under different mesh densities, we define the following error function,

$$\mathrm{Err}=\frac{1}{M}\sum_{i=1}^{M}\frac{\left|n_{eff,i}^{2(FEM)}-n_{eff,i}^{2(REF)}\right|}{n_{eff,i}^{2(REF)}}, \tag{6}$$

where M is the number of eigenmodes, $n_{eff,i}^{(FEM)}$ represents the effective refractive index of the i-th eigenmode for the method to be compared, and $n_{eff,i}^{(REF)}$ represents the reference effective refractive index of the i-th eigenmode. It is worth emphasizing that by defining the error in this way, the offset between the calculated effective refractive and the reference effective refractive makes the change in the defined error more significant, which helps to validate the accuracy of our approach.

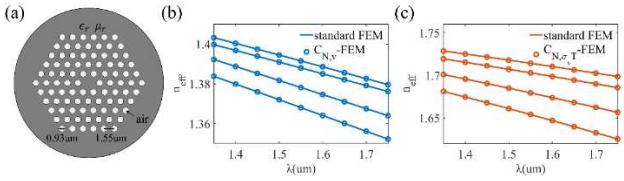

Fig. 1. The structure of photonic crystal waveguide and dispersion curve. (a) the structure of optical waveguides. (b). dispersion curve when the core is isotropic material. (c). dispersion curve when the core is anisotropic material.

To verify the robustness of our method, we calculate the dispersion curves of more complex photonic crystal waveguides. The photonic crystal waveguide structures are shown in Fig. 1. When $\epsilon_r=2.1$ and $\mu_{r,1}=1$, indicating the medium is isotropic media, the photonic crystal waveguide possesses $C_{6,v}$ point group symmetry, which is suitable for modal analysis using $C_{N,v}$ -FEM. When $\epsilon_r=2.1$ and $\mu_r=\begin{bmatrix}1 & -0.51i & 0\\ 0.51i & 1 & 0\\ 0 & 0 & 1\end{bmatrix}$, meaning the medium is an anisotropic medium satisfying $\hat{S}\mu_r^*\left(\hat{S}^{-1}\mathbf{r}\right)\hat{S}^{-1}=\mu_r(r)$, so the optical waveguide has MT symmetry and C_6 point group symmetry, enabling modal analysis using $C_{N,\sigma_v T}$-FEM. The dispersion curves of photonic crystal waveguides with the mesh density of 8 and wavelengths ranging from 1.35um to 1.75um are calculated using both our method and standard FEM. The results of dispersion curve are shown in Fig. 1b and Fig. 1c, corresponding to the medium being isotropic and anisotropic materials, respectively, where it can be observed that our method yields consistent results with standard FEM even for complex structured waveguides.

Fig. 2 shows accuracy and efficiency improvement of standard FEM, σ_v -FEM, C_N -FEM and our method under different mesh densities. All FEM methods calculate the first 200 eigenmodes of waveguides and compute the relative error with respect to the reference results using (6). Our method requires multiple calculations, so the computational

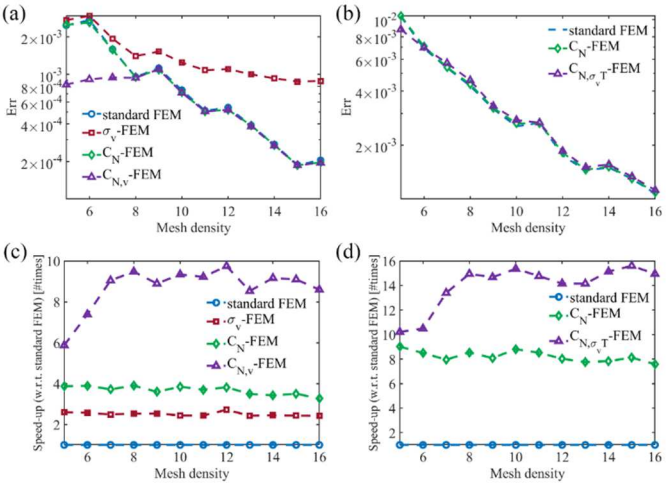

Fig. 2. Accuracy and efficiency improvement of different FEM methods relative to standard FEM. (a) and (c) represent the results of the photonic crystal waveguide with $C_{6,v}$ point group symmetry. (b) and (d) represent the results of the photonic crystal waveguide with C_6 point group symmetry and mirror time-inverse symmetry.

time is the sum of several sub-eigenvalue problem computation times. As shown in Fig. 2a and 2b, the calculation accuracy of the structure in Fig. 1a is illustrated. The structure with $\mu_r=\begin{bmatrix}1 & -0.51i & 0\\ 0.51i & 1 & 0\\ 0 & 0 & 1\end{bmatrix}$ lacks mirror symmetry, so only the standard FEM, C_N-FEM, and the method proposed in this paper are used. Our method demonstrates consistent calculation accuracy with C_N-FEM and standard FEM. Fig. 2c and 2d are plotted taking standard FEM as the baseline at the same mesh density to showcase the relative speed improvement achieved by different methods compared to standard FEM. Compared to standard FEM, our method achieves about an order of magnitude improvement in computational efficiency, and compared to C_N-FEM, our method achieves approximately double the improvement. These results indicate that our method also possesses a significant advantage in computational efficiency when analyzing eigenmode of complex waveguide structures.

Our method classifies the eigenmodes based on symmetry. Therefore, we discuss the number of eigenmodes calculated for different classifications. In $C_{N,v}$-FEM, when q=0, $\chi(\sigma_v)$=1/-1 corresponds to eigenmode A_1/A_2; when q=3, $\chi(\sigma_v)$=1/-1 corresponds to eigenmode B_1/B_2; q=1/5 corresponds to eigenmode E_1; q=2/4 corresponds to eigenmode E_2. In C_{N,σ_vT}-FEM, q=0 corresponds to eigenmode A, q=3 corresponds to eigenmode B, q=1/5 corresponds to eigenmode E_1, and q=2/4 corresponds to eigenmode E_2. It should be noted that due to the lack of time inversion symmetry in the structure with $\mu_r=\begin{bmatrix}1 & -0.51i & 0\\ 0.51i & 1 & 0\\ 0 & 0 & 1\end{bmatrix}$, the degenerate eigenmodes protected by symmetry are broken. However, in order to correspond to character label, we still classify q=1/5 as the E_1 eigenmode and q=2/4 as the E_2 eigenmode. Calculate the first few hundred eigenmodes and count the number of different eigenmodes of classification. The results are shown in Table II. It can be seen that the proportions of different classification eigenmodes are fixed. Our method can classify eigenmodes based on symmetry and directly calculate eigenmodes of different classifications, which provides convenience for analyzing waveguide modes.

TABLE II. NUMBER OF EIGENMODES IN DIFFERENT CLASSIFICATIONS

	A_1	A_2	B_1	B_2	E_1	E_2
$C_{N,v}$-FEM	17	17	17	17	66	66
Standard FEM	200					
$C_{N,v}$-FEM	33	34	34	32	134	133
Standard FEM	400					
$C_{N,v}$-FEM	50	51	49	49	201	200
Standard FEM	600					
$C_{N,v}$-FEM	67	67	66	66	266	268
Standard FEM	800					

	A	B	E_1	E_2
C_{N,σ_vT}-FEM	33	33	67	67
Standard FEM	200			
C_{N,σ_vT}-FEM	67	65	134	134
Standard FEM	400			
C_{N,σ_vT}-FEM	99	100	201	200
Standard FEM	600			
C_{N,σ_vT}-FEM	132	134	265	269
Standard FEM	800			

IV. CONCLUSION

Our study systematically investigates the utilization of point group symmetry and space-time symmetry in computing the vector eigenmodes of optical waveguides through FEM, employing group theory. We provide a theoretical framework for constructing combined symmetric boundary, which includes and extends the existing theories. When incorporating multiple symmetries, we distinguish two situations: employing only point group symmetry and combining point group symmetry with space-time symmetry. Our method classifies and solves modes based on symmetry, allowing for the calculation of specific LP modes only, and obtaining the characteristics of the electric and magnetic field components of the modes in advance. To demonstrate the effectiveness of our proposed method, we provide numerical cases for both $C_{N,v}$-FEM and C_{N,σ_vT}-FEM. In both instances, our approach yields comparable computational precision to existing methods while significantly enhancing computational efficiency. Our method is not only applicable to FEM, but also very easy to apply to other numerical methods, such as FDTD and transfer matrix method. Considering the fundamental role of group theory methods in optics and computational photonics, we argue that our work, which employs multiple symmetries to compute the vector eigenmodes of symmetric photonic structures, holds broad applicability and contributes vital information for eigenmode classification. Therefore, our work aids in the design and analysis of photon devices exhibiting multiple degrees of symmetry.

ACKNOWLEDGMENT

The preferred spelling of the word “acknowledgment” in America is without an “e” after the “g”. Avoid the stilted expression “one of us (R. B. G.) thanks ...”. Instead, try “R. B. G. thanks...”. Put sponsor acknowledgments in the unnumbered footnote on the first page.

REFERENCES

[1] X. Zhang *et al.*, “Symmetry-breaking-induced nonlinear optics at a microcavity surface,” *Nat. Photonics*, vol. 13, no. 1, Art. no. 1, Jan. 2019, doi: 10.1038/s41566-018-0297-y

[2] D. Bird, “Mode symmetry in microstructured fibres revisited,” *Opt. Express*, vol. 26, no. 24, pp. 31454–31463, Nov. 2018, doi: 10.1364/OE.26.031454

[3] W. Liu *et al.*, “Circularly Polarized States Spawning from Bound States in the Continuum,” *Phys. Rev. Lett.*, vol. 123, no. 11, p. 116104, Sep. 2019, doi: 10.1103/PhysRevLett.123.116104

[4] W. Chen, Z. Xiong, J. Xu, and Y. Chen, "Generalized coupled-mode formalism in reciprocal waveguides with gain, loss, anisotropy, or bianisotropy," *Phys. Rev. B*, vol. 99, no. 19, p. 195307, May 2019, doi: 10.1103/PhysRevB.99.195307

[5] R. Otin, J. Verpoorte, and H. Schippers, "Finite Element Model for the Computation of the Transfer Impedance of Cable Shields," *IEEE Trans. Electromagn. Compat.*, vol. 53, no. 4, pp. 950–958, Nov. 2011, doi: 10.1109/TEMC.2011.2146257

[6] G. Garcia-Contreras, J. Córcoles, and J. A. Ruiz-Cruz, "Degeneracy-Discriminating Modal FEM Computation in Higher Order Rotationally Symmetric Waveguides," *IEEE Trans. Antennas Propag.*, vol. 69, no. 11, pp. 8003–8008, Nov. 2021, doi: 10.1109/TAP.2021.3083790

[7] G. Garcia-Contreras, J. Córcoles, and J. A. Ruiz-Cruz, "Rigorous Modal Characterization of First- and Second-Order Symmetric Waveguides Using Specular Periodic Boundary Conditions in 2D-FEM," *IEEE Trans. Antennas Propag.*, vol. 70, no. 11, pp. 10800–10810, Nov. 2022, doi: 10.1109/TAP.2022.3209222

[8] V. Heine, "Group Theory: Application to the Physics of Condensed Matter," *Phys. Today*, vol. 61, no. 11, pp. 57–58, Nov. 2008, doi: 10.1063/1.3027994

[9] T. Inui, Y. Tanabe, and Y. Onodera, *Group theory and its applications in physics*, vol. 78. Springer Science & Business Media, 2012.

[10] K. Shao, Z.-T. Cai, H. Geng, W. Chen, and D. Y. Xing, "Cyclotron quantization and mirror-time transition on nonreciprocal lattices," *Phys. Rev. B*, vol. 106, no. 8, p. L081402, Aug. 2022, doi: 10.1103/PhysRevB.106.L081402